

## PDF hosted at the Radboud Repository of the Radboud University Nijmegen

The following full text is a publisher's version.

For additional information about this publication click this link.

<http://hdl.handle.net/2066/24513>

Please be advised that this information was generated on 2017-12-05 and may be subject to change.

# New Mutations in the AQP2 Gene in Nephrogenic Diabetes Insipidus Resulting in Functional but Misrouted Water Channels

SABINE M. MULDER<sup>\*</sup>, NINE V.A.M. KNOERS<sup>†</sup>, ANGENITA F. VAN LIEBURG<sup>‡</sup>, LEO A.H. MONNENS<sup>‡</sup>, ERNST LEUMANN<sup>§</sup>, ELKE WÜHL<sup>||</sup>, EDITH SCHOBER<sup>¶</sup>, JOHAN P.L. RIJSS<sup>\*</sup>, CAREL H. VAN OS<sup>\*</sup> and PETER M.T. DEEN<sup>\*</sup>

<sup>\*</sup>Department of Cell Physiology, University of Nijmegen, Nijmegen, The Netherlands; <sup>†</sup>Department of Human Genetics, University of Nijmegen, Nijmegen, The Netherlands; <sup>‡</sup>Department of Pediatrics, University of Nijmegen, Nijmegen, The Netherlands; <sup>§</sup>Universitäts-Kinderklinik Zurich, Zurich, Switzerland; <sup>||</sup>Department of Pediatrics, University of Heidelberg, Heidelberg, Germany; <sup>¶</sup>Universitäts-Kinderklinik Wien, Vienna, Austria.

**Abstract.** Nephrogenic diabetes insipidus (NDI) is characterized by the inability of the kidney to concentrate urine in response to vasopressin. The autosomal recessive form of NDI is caused by mutations in the AQP2 gene, encoding the vasopressin-regulated water channel of the kidney collecting duct. This report presents three new mutations in the AQP2 gene that cause NDI, resulting in A147T-, T126M-, or N68S-substituted AQP2 proteins. Expression of the A147T and T126M mutant AQP2 proteins in *Xenopus* oocytes revealed a relatively small, but significant increase in water permeability, whereas the water permeability of N68S expressing oocytes was not increased. cRNA encoding missense and wild-type AQP2 were

equally stable in oocytes. Immunoblots of oocyte lysates showed that only the A147T mutant protein was less stable than wild-type AQP2. The mutant AQP2 proteins showed, in addition to the wild-type 29-kd band, an endoplasmic reticulum-retarded form of AQP2 of approximately 32 kd. Immunoblotting and immunocytochemistry demonstrated only intense labeling of the plasma membranes of oocytes expressing wild-type AQP2. In summary, two mutant AQP2 proteins encoded in NDI are functional water channels. Therefore, the major cause underlying autosomal recessive NDI is the misrouting of AQP2 mutant proteins. (J Am Soc Nephrol 8: 242–248, 1997)

Aquaporins are selective water channels and form a subset of the MIP family of intrinsic membrane proteins. In the kidney, four aquaporins (AQP 1 through 4) (1–6) have been identified and are postulated to be involved in reabsorption and concentration of the glomerular filtrate. AQP1 is constitutively expressed in the proximal tubule and descending limb of Henle, and is localized to apical and basolateral membranes (7). AQP2 is the vasopressin-regulated water channel of principal cells of the collecting duct (2). In the absence of vasopressin, AQP2 is localized in vesicles in the subapical region of the cell. Upon binding of vasopressin to its V<sub>2</sub> receptor, AQP2 water channels are inserted into the apical membrane, conferring a high water permeability to this membrane. Upon removal of vasopressin, the channels are retrieved by endocytosis (8–12). AQP3 and AQP4 are localized to the basolateral membrane of principal cells of the collecting duct, and are suggested to function as an exit pathway for water (13). So far, only AQP2 has been shown to be involved in diseases. Individuals who lack functional

AQP1 do not exhibit clinical symptoms, which raised questions about the physiological significance of AQP1 (14). Mutations in AQP3 and AQP4 have not been identified so far. Mutations in the AQP2 gene, however, have been shown to be the cause of the autosomal recessive form of nephrogenic diabetes insipidus (NDI), a severe disease that is characterized by the inability of the kidney to concentrate urine in response to vasopressin (15,16). In the majority of patients, NDI is caused by a mutation in the V<sub>2</sub> receptor gene, and is inherited as a X-linked recessive trait. In approximately 10% of the families, NDI has shown a non-X-linked pattern of inheritance. So far, a one-nucleotide deletion and three mutations coding for missense mutations in AQP2 have been reported as a cause of NDI in some of these families (15,16). Upon expression in *Xenopus* oocytes, the missense AQP2 proteins with a G64R, R187C, or S216P substitution were unable to increase the water permeability (Pf) of oocytes, whereas expression of wild type AQP2 increased Pf values more than 10-fold. Further studies revealed that the mutant AQP2 proteins were impaired in their cellular routing (17). Consequently, it remained undecided whether these mutations resulted in non-functional water channels, since they did not reach the plasma membrane.

In the study presented here, we report three additional NDI patients who are homozygous for mutations in the AQP2 gene. In addition, we performed functional analyses of the mutant AQP2 proteins in oocytes and concluded that two mutations result in functional but misrouted water channels.

Received October 21, 1996. Accepted November 25, 1996.

Correspondence to Dr. Peter M.T. Deen, 162 Department of Cell Physiology, University of Nijmegen, P.O. Box 9101, 6500 HB Nijmegen, The Netherlands.

1046-6673/9802-0242\$03.00/0

Journal of the American Society of Nephrology

Copyright © 1997 by the American Society of Nephrology

## Materials and Methods

### Patients

The three patients investigated in this study come from three separate families from different ethnic origin. In all three families, the parents of the patients are consanguineous.

Family 1 is of Austrian descent. The male proband (Patient 1) was admitted to the hospital at the age of 3 months with signs of dehydration, including recurrent fever and hypernatremia (serum sodium concentration, 164 mmol/L). On admission, urinary osmolality was very low (50 mosmol/kg) and did not increase after a water-deprivation test or after the administration of arginine vasopressin. At present, at the age of 18 yr, he has a polyuria and polydipsia of approximately 13 L/day (no medication). In his older sister, a diagnosis of diabetes insipidus was made at the age of a few months. Data on a water-deprivation test or a DDAVP (deamino-8-D-arginine vasopressin; Minrin®) test were not available in her medical record. She has been treated, however, with Minrin® without a reduction in urinary volume. Now, as an adult, she has a fluid intake of approximately 13 L/day (no medication).

Family 2 comes from Sri Lanka. The male proband (Patient 2) was referred at the age of 5 months because of intermittent high fever, weakness, irritability, and weight loss. The diagnosis of NDI was based on the presence of a high serum sodium concentration (186 mmol/L), a low urinary osmolality (173 mosmol/kg), and unresponsiveness to DDAVP. Therapy with hydrochlorothiazide proved very difficult despite tube feeding and was complicated by intermittent bulging fontanel, fever, and vomiting. The boy failed to thrive and showed muscular hypotonia and delayed psychomotor development. At the age of 13 months he was readmitted with high fever, seizures, and hypernatremia (173 mmol/L), followed by coma. He succumbed two weeks later. MRI and necropsy revealed severe brain lesions with necrosis of basal ganglia. Eight months later NDI was diagnosed in the younger brother at the age of 1 wk based on elevated serum sodium (147 mmol/L) and low urinary osmolality (107 mosmol/kg). At present, at the age of 2 yr, his psychomotor development is adequate but there is slight muscular hypotonia. Fluid intake is 2 L/day.

Family 3 is Turkish by descent. In the female proband (Patient 3), the diagnosis diabetes insipidus was made at the age of 6 wk when she was admitted to the children's hospital with failure to thrive and signs of dehydration, including fever, and hypernatremia (serum sodium concentration, 162 mmol/L). Urinary osmolality was low (82 mosmol/kg) but increased to 236 mosmol/kg after water deprivation and to 450 mosmol/kg after administration of arginine vasopressin, suggesting a diagnosis of nephrogenic diabetes insipidus with partial resistance to vasopressin. However, at the age of 18 months, a control vasopressin test showed a rise of urine osmolality to only 239 mosmol/kg. According to the parents, two sons of the sister of the paternal grandmother, at that time 7 and 8 yr old, both suffered from a similar disease. Further investigation revealed that they both had NDI with total resistance to vasopressin. All three patients have been treated with the combination indomethacin-hydrochlorothiazide, which was replaced for amiloride and Minrin® in the proband at the age of 4 yr. Despite treatment, she still had a fluid intake of approximately 4 L/day at that age.

### DNA Amplification and Sequence Analysis of Patients

Genomic DNA was isolated by the salt-extraction technique. Primers used for amplification of the AQP2 coding regions and for cycle sequencing were as described elsewhere (15). PCR conditions were 1 min at 92°C, 1.5 min at 60°C, and 1.5 min at 72°C for 30 cycles. Cycle sequencing reactions were performed on both DNA strands, and sequences were analyzed on an automated fluorescence-based Applied Biosystems model 373A DNA sequencing system.

### DNA Constructs and Transcription

To introduce the A147T mutation in our AQP2 expression construct (pT7TsAQP2), exon 2 of the AQP2 gene was amplified from genomic DNA of Patient 1. A 66-base pair (bp) *SacI-SmaI* fragment containing the G to A transition at position 533 was isolated by gel electrophoresis. For the T126M mutation, genomic DNA of Patient 2 was amplified using primers flanking the coding region of exon 2, and a 43-bp *DdeI-SacI* fragment was isolated, containing the C to T transition at position 471. For the N68S mutation, exon 1 of the AQP2 gene was amplified from genomic DNA of Patient 3, and a 144-bp *ApaI-SacII* fragment containing the A to G transition at position 297 was isolated. These fragments were inserted into the corresponding sites of pT7TsAQP2 and clones that were identical to the wild-type (wt) AQP2 cDNA sequence, except for the described mutations, were selected by sequence analysis (18). These constructs were linearized by *SalI* and capped RNA transcripts were synthesized *in vitro* using T7 RNA polymerase according to Promega's (1991) Protocols and Principles guide, except that 1-mM final concentrations of NTP and 7-methyl-di-guanosine triphosphate were used. The cRNA were purified and dissolved in diethyl pyrocarbonate-treated water. The integrity of the RNA was checked by agarose gel electrophoresis and the concentration was determined spectrophotometrically.

### Water Permeability

*Xenopus laevis* oocytes were isolated, injected with 10 ng cRNA and analyzed after 3 days in a swelling assay as described before (15). Oocyte swelling was performed at 22°C after transfer from 200 mosM to 70 mosM (wt AQP2 expressing oocytes) or 200 mosM to 20 mosM (water-injected control oocytes and mutant AQP2 expressing oocytes).

### Northern Blot Analysis

At the day of injection and 3 days after injection, RNA was isolated from six oocytes according to Chomczynski and Sacchi (19). RNA equivalents of three oocytes were loaded onto a 2.2 M formaldehyde, 1% (wt/vol) agarose gel. Electrophoresis, blotting, and hybridization conditions were as described (20). A 850-bp *EcoRI* cDNA fragment encoding human AQP2 (15) was labeled with [ $\alpha$ -<sup>32</sup>P] dCTP by random priming (21) and was used as a probe. The relative amount of mRNA loaded onto the gel was assessed by hybridization of the same blot with a probe of a 780-bp *EcoRI-BamHI* cDNA fragment coding for *Xenopus laevis* Histon H3 (22) and subsequent scanning of the autoradiographic signals with an LKB Ultrascan XL laser densitometer (Pharmacia Biotech, Uppsala, Sweden).

### Immunoblotting

To determine the stability of mutant and wt AQP2 proteins, eight oocytes were homogenized in 20  $\mu$ L buffer A per oocyte (20 mM Tris [pH 7.4], 5 mM MgCl<sub>2</sub>, 5 mM NaHPO<sub>4</sub>, 1 mM EDTA, 1 mM dithiothreitol [DTT], 1 mM phenylmethyl sulfonyl fluoride [PMSF], 5  $\mu$ g/mL leupeptin and pepstatin, 80 mM sucrose) at 4°C at 1, 2, and 3 days after injection. Subsequently, the lysates were centrifuged twice for 10 min at 125 g to remove yolk proteins. At the third day after injection, a fraction enriched for plasma membranes was isolated from 25 oocytes according to Wall and Patel (23).

Lysates or plasma membranes equivalent to 0.1 oocyte or eight oocytes, respectively, were denatured for 30 min at 37°C in sample buffer (2% sodium dodecyl sulfate [SDS], 50 mM Tris (pH 6.8), 12% glycerol, 0.01% Coomassie Brilliant Blue, 100 mM DTT), electrophoresed through a 12% SDS-polyacrylamide gel (24) and transferred to a nitrocellulose membrane as described (15). Efficiency of protein transfer was checked by staining the membrane with Ponceau Red. For immunodetection, the membrane was incubated with a 1:10,000 dilution of an

affinity-purified polyclonal antibody directed against the 15 C-terminal amino acids of rat AQP2 (17). As a secondary antibody, a 1:5,000 dilution of affinity-purified goat-anti-rabbit IgG conjugated to horse radish peroxidase (Sigma Immuno Chemicals, St. Louis, MO) was used. Proteins were visualized using enhanced chemiluminescence (Boehringer Mannheim). When appropriate, the 29- and 32-kd AQP2 bands of the third day were scanned as described above.

### Immunocytochemistry

At 3 days after injection, remaining vitelline membranes were removed and oocytes were incubated for 1 h in 1% wt/vol paraformaldehyde fixative (PLP) (25), dehydrated, and embedded in paraffin. After being blocked with 10% goat serum in Tris-buffered saline (TBS), the sections were incubated O/N at 4°C with the polyclonal AQP2 diluted 1:500 in 10% goat serum in TBS. After three washes for 10 min in TBS, the sections were incubated for 1 h in a 1:100 dilution of goat-anti-rabbit IgG coupled to fluorescein isothiocyanate (Sigma Immuno Chemicals). The sections were again washed three times for 10 min, dehydrated by washing in 70% to 100% ethanol, and mounted in mowiol 4-88, containing 2.5% NaN<sub>3</sub>. Photographs were taken with a Zeiss Axioskop (Zeiss, Oberkochen, Germany) with epifluorescent illumination with an automatic camera using Kodak EPH P1600X films (Eastman Kodak, Rochester, NY).

### Results

From three NDI patients, in whom a V<sub>2</sub> receptor defect was either excluded or unlikely, we amplified and sequenced the four exons of the AQP2 gene. All patients were found to be homozygous for three different missense mutations. In Patient 1, a G533A transition was found in exon 2, leading to a substitution of an alanine for threonine (A147T). In Patient 2, a C471T transition in exon 2 leads to a threonine to methionine substitution (T126M). The AQP2 gene of patient 3 showed a A297G transition in exon 1, which results in a substitution of an asparagine for a serine (N68S) in one of the most conserved regions of the MIP family proteins (26) (Figure 1).

The asymptomatic parents and a healthy brother and sister of Patient 1 were shown to be heterozygous for the A147T mutation; another asymptomatic sister appeared to be homozygous for the normal allele. As expected, the affected brother of Patient 2 appeared homozygous for the T126M mutation as well, whereas their asymptomatic parents were both shown to be heterozygous for that mutation. DNA of an elder healthy brother was not available for testing. Sequencing of exon 1 in the two affected male family members of Patient 3 revealed that they both were homozygous for the N68S mutation. The asymptomatic parents, an asymptomatic sister of the father and the paternal grandparents of Patient 3, as well as the mother of the two other patients in family 3, were all shown to be heterozygous for the N68S mutation. The data are consistent with co-segregation of the mutant AQP2 allele with the disease and with autosomal recessive inheritance of NDI in these families.

To test whether these mutant AQP2 proteins are functional water channels, PCR fragments containing the mutations were cloned into the AQP2 expression vector and transcripts were injected into *Xenopus* oocytes. Three days later, water permeability measurements revealed that the water permeability (Pf ± SE) of oocytes expressing the N68S mutant (8.3 ± 1.9

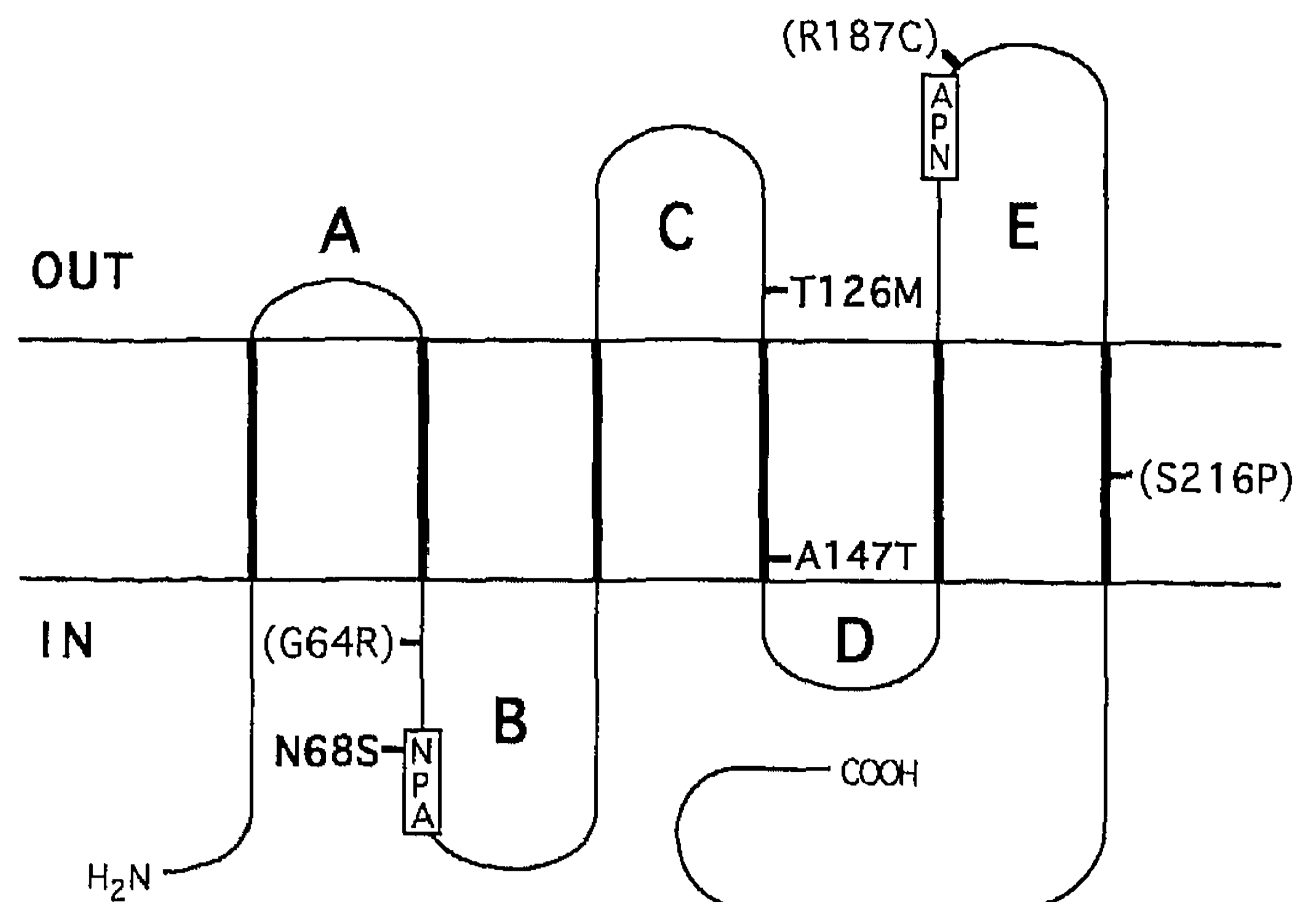


Figure 1. Proposed membrane topology of AQP2. The three amino acid substitutions as coded for by the AQP2 genes of the three NDI patients and the conserved NPA boxes are indicated. The previously reported amino acid substitutions in NDI patients (15,16) are shown between brackets.

$\mu\text{m/s}$ ) was not different from water-injected control oocytes ( $8.9 \pm 2.2 \mu\text{m/s}$ ), whereas oocytes expressing the T126M ( $41.4 \pm 3.8 \mu\text{m/s}$ ) or A147T ( $46.2 \pm 2.7 \mu\text{m/s}$ ) AQP2 proteins showed a significantly increased water permeability when compared with water-injected control oocytes.

The water permeability of wild-type (wt) AQP2 injected oocytes was  $275 \pm 9.7 \mu\text{m/s}$  (Figure 2). The low or absent water permeability of mutant AQP2 proteins in *Xenopus* oocytes could be caused by (1) a low stability of the mutant cRNAs in *Xenopus* oocytes; (2) a low stability of the mutant AQP2 proteins in oocytes; (3) an impairment of the routing of the mutant AQP2 proteins to the plasma membrane; and/or (4) a mutant AQP2 protein that is a non-functional water channel.

To test for differences in stability of wt and mutant cRNA, RNA isolated from oocytes directly after, and 3 days after

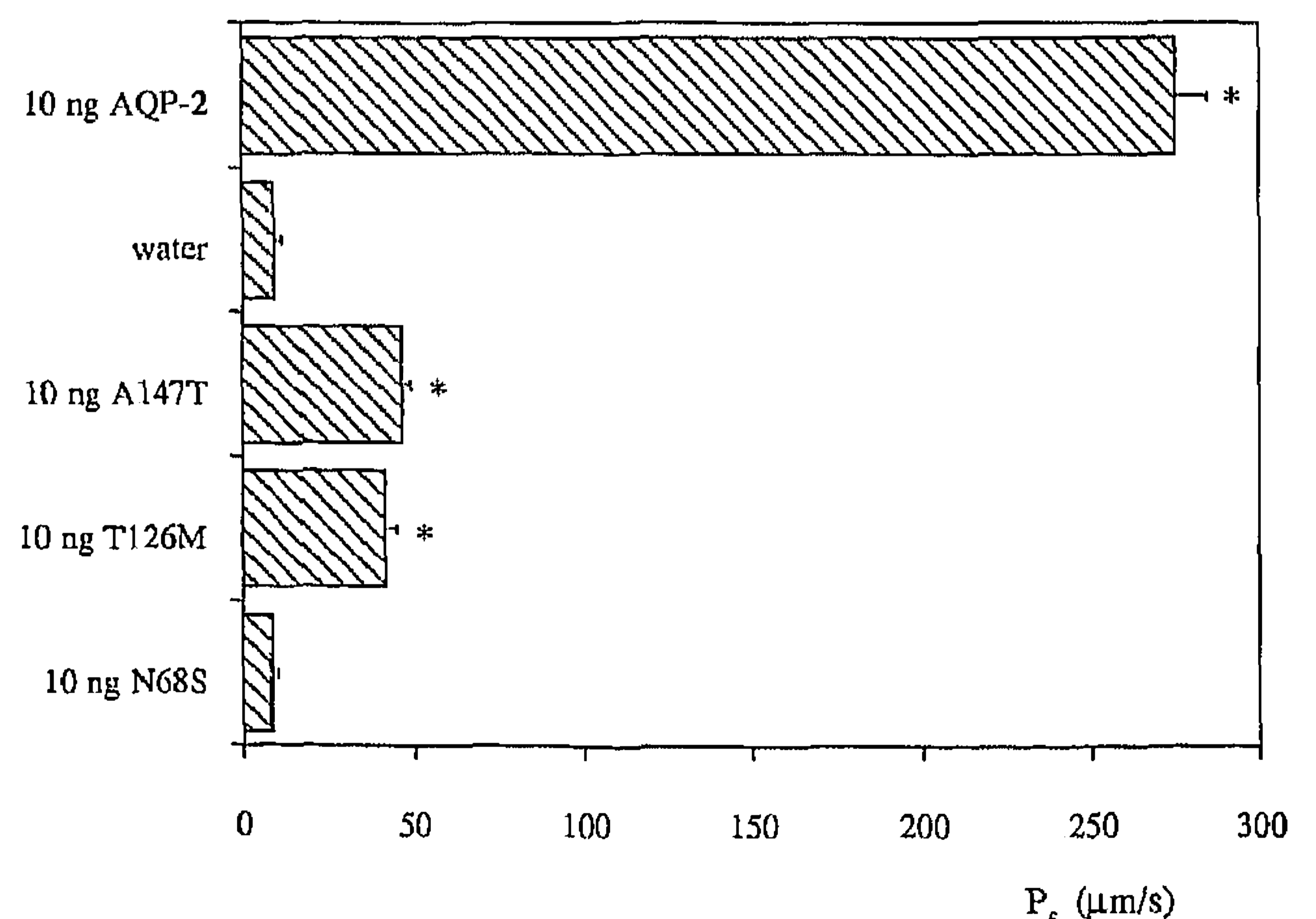


Figure 2. Osmotic water permeability (Pf) of oocytes 3 days after injection of water or 10 ng cRNA encoding wt, A147T, T126M, or N68S AQP2. Mean and SE of at least 45 oocytes from six different experiments are shown (\*, significantly increased above water-injected control oocytes;  $P < 0.01$ ).

injection was subjected to Northern blot analysis. A specific signal with our human AQP2 cDNA probe was only obtained in lanes loaded with RNA isolated from AQP2 cRNA-injected oocytes (Figure 3). After normalization for the amounts of RNA loaded by hybridization with a *Xenopus* Histon H3 probe, the amounts of wt and mutant AQP2 cRNAs were comparable.

To compare the size and stability of mutant and wt AQP2 proteins, oocyte lysates were prepared 1, 2, and 3 days after injection and were subjected to immunoblotting using AQP2 antibodies (Figure 4). Ponceau Red staining of the immunoblot showed that equal amounts of protein were loaded (not shown). Chemiluminescence detection revealed a band of 29-kd present in all lanes loaded with AQP2 protein, except in the lane loaded with water-injected control oocytes. In the lanes loaded with mutant AQP2 protein an additional band of approximately 32 kd was present. Densitometric scanning of the bands from the third day samples revealed that the stability of the T126M and N68S mutants and wt AQP2 were equal, whereas the stability of the A147T mutant was less than 10% of wt AQP2.

To determine the plasma membrane expression of wt and mutant AQP2 proteins, a fraction enriched for plasma membranes was subjected to immunoblotting (Figure 5). Only in the membrane fraction of oocytes expressing wt AQP2 was a clear 29-kd band visible, whereas no AQP2 protein could be detected in the membrane fractions of AQP2 mutants. To visualize the location of AQP2 proteins, immunocytochemistry was performed on injected oocytes (Figure 6). Staining with the AQP2 antibody revealed a clear, intense staining of the plasma membrane of oocytes expressing wt AQP2 (Figure 6A), whereas oocytes expressing mutant AQP2 proteins showed a very weak staining of the plasma membrane, with a more pronounced labeling of the cytoplasm (Figure 6B-D). The water-injected control oocytes showed no staining (Figure 6E).

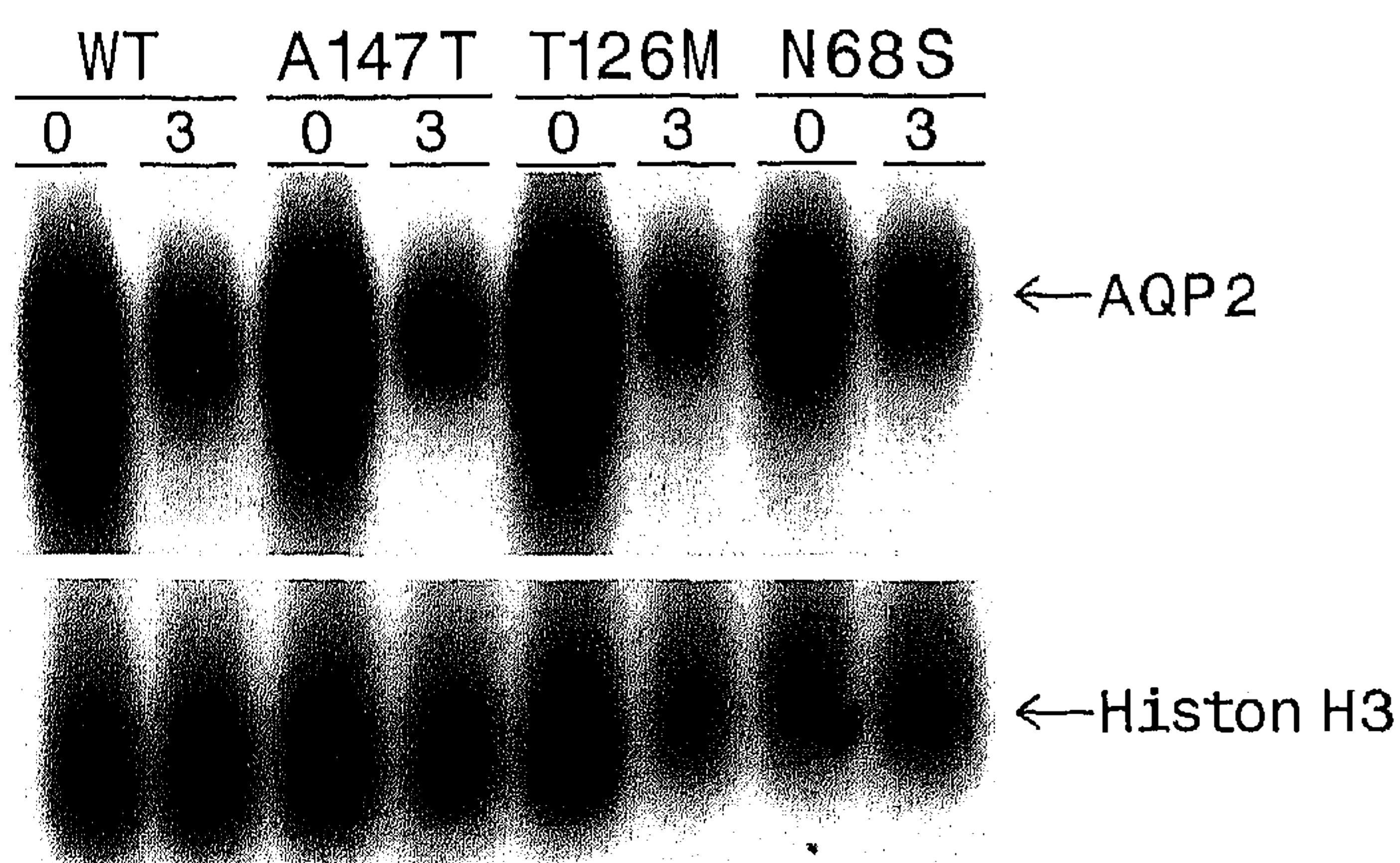


Figure 3. Northern blot analysis of the stabilities of cRNA encoding wt, A147T, T126M, or N68S AQP2 in *Xenopus* oocytes. At the day of injection and 3 days after injection, RNA was isolated from six oocytes. An equivalent of three oocytes was blotted and RNA was visualized using a human AQP2 cDNA probe (upper panel). For normalization of the amount of RNA loaded, the blot was hybridized with a *Xenopus* histon H3 probe (lower panel).

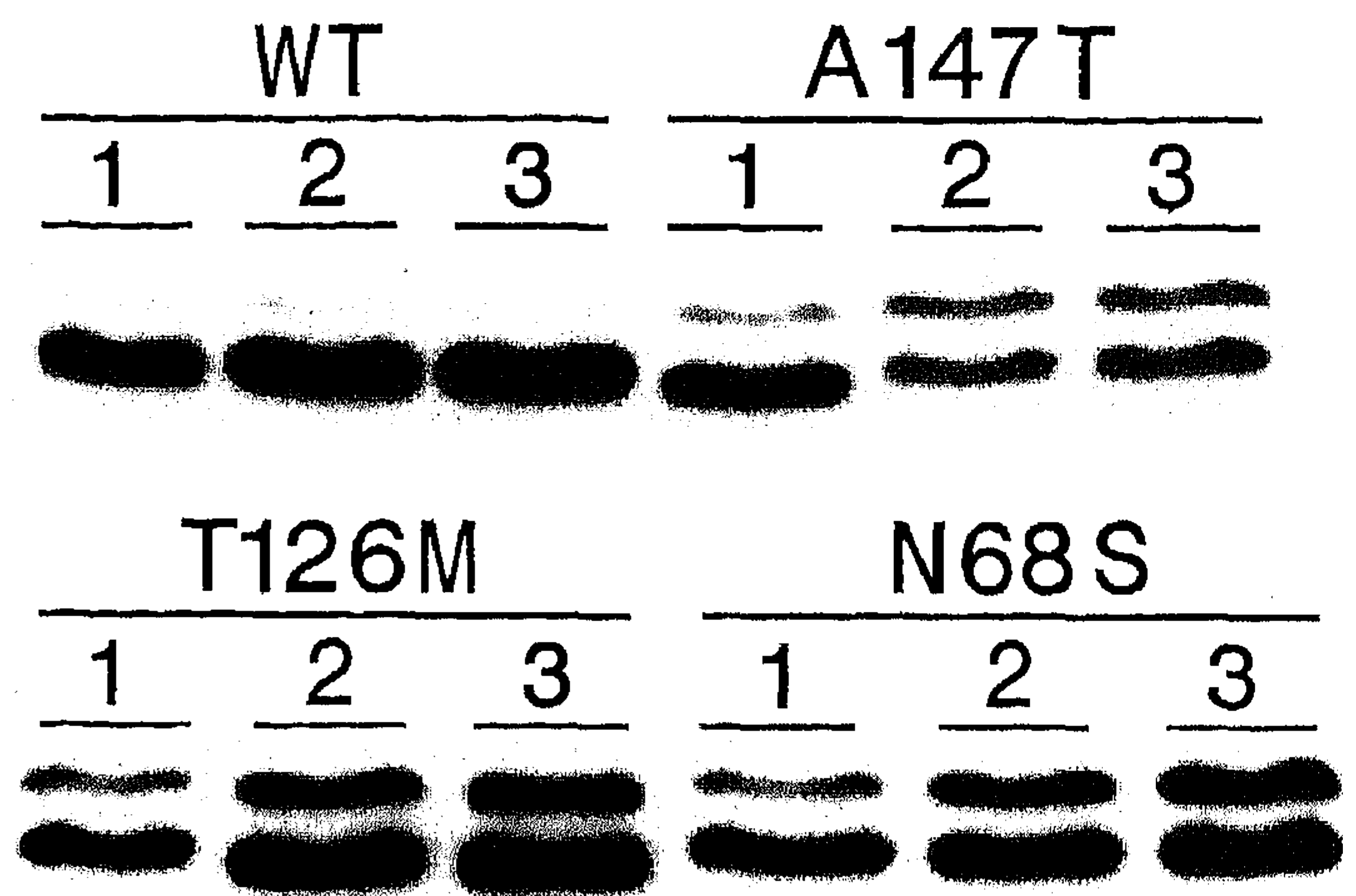


Figure 4. Immunoblot analysis of AQP2 proteins. At 1, 2, and 3 days after injection, lysates were prepared from eight oocytes injected with water or cRNA encoding wt, A147T, T126M, or N68S AQP2. Equivalents of 0.1 oocyte were separated by SDS-PAGE and blotted. AQP2 proteins were visualized by chemiluminescence using AQP2 antibodies as a first antibody and anti-rabbit IgG, conjugated to peroxidase, as a second antibody.

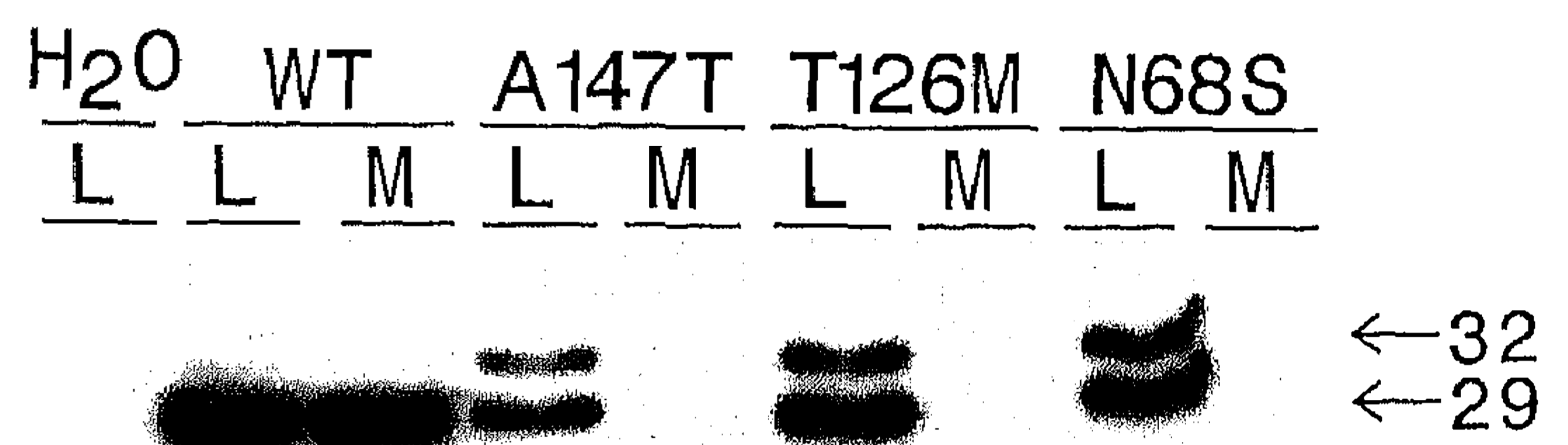
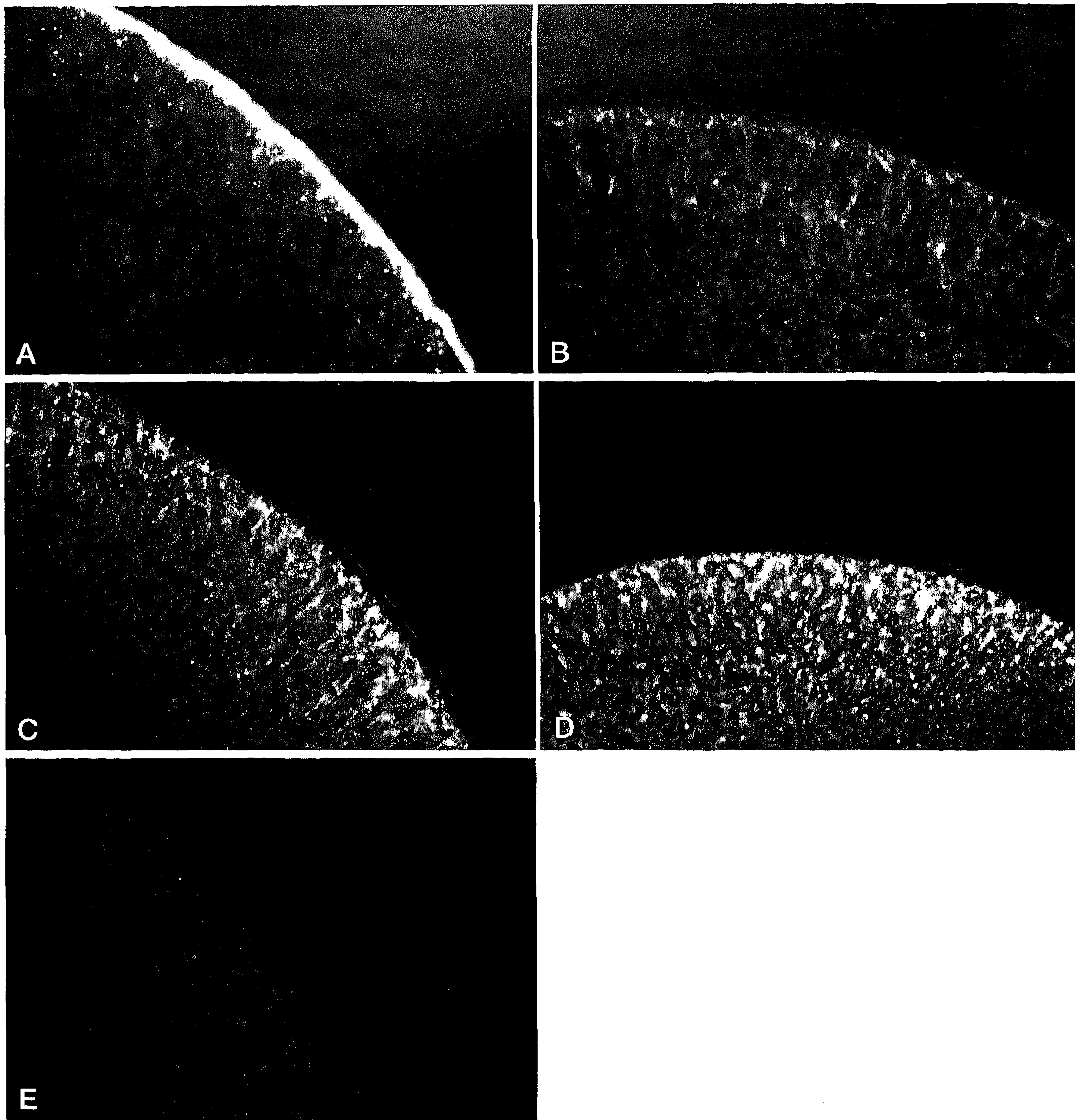


Figure 5. Immunoblot analysis of lysates and a fraction enriched for plasma membranes of oocytes. Lysates (L) and plasma membranes (M) were prepared 3 days after injection of water or cRNA encoding wt, A147T, T126M, or N68S AQP2. Equivalents of 0.1 oocyte (L) or eight oocytes (M) were separated by SDS-PAGE and immunoblotted as described in the legend of Figure 4.

## Discussion

The discovery of mutations in the  $V_2$  receptor gene, located on the X-chromosome, explained the cause of NDI in a majority of the patients (27), but not in all. Some of these unexplained NDI cases appeared to segregate as an autosomal recessive trait, and mutations in the  $V_2$  receptor coding region could often be excluded in these cases. Therefore, the involvement of a second gene causing NDI was likely. In search for proteins involved in the cascade of events between the binding of vasopressin to the  $V_2$  receptor at the basolateral membrane and the reabsorption of water at the apical membrane of the collecting duct cell, the cloning of the rat AQP2 water channel, which is exclusively expressed in the collecting duct (2), attracted attention. The AQP2 gene was assigned to chromosome 12, region q12-q13, and was therefore a likely candidate (28). The subsequent identification of mutations in the AQP2 gene in some of these NDI patients provided a definitive proof for a second gene defect in NDI (15,16).

Here we report three new missense mutations in the AQP2 gene of three NDI patients coding for a A147T-, T126M-, or N68S-substituted AQP2 protein. Expressed in *Xenopus* oo-



**Figure 6.** Sections of oocytes injected with cRNA encoding wt (A), A147T (B), T126M (C), or N68S (D) AQP2. As a negative control, water-injected control oocytes were used (E). The sections were incubated with AQP2 antibodies and visualized by FITC-conjugated anti-rabbit immunoglobulins.

ocytes, the N68S mutant AQP2 was non-functional (Figure 2). This could be anticipated, because the substituted amino acid is part of the NPA box in loop B, which forms, together with a second NPA box in loop E, the most conserved amino acid sequence of the MIP-family (26). Unlike the N68S-substituted protein and previously reported AQP2 mutants (G64R, R187C, and S216P) (15,16), the A147T and T126M AQP2 mutant proteins were functional. The alanine at position 147 is also

well-conserved among the MIP family members (26). The observed water permeability of the oocytes expressing the A147T and T126M AQP2 proteins was, however, much lower than that of oocytes expressing wt AQP2.

To find an explanation for the reduced Pf of oocytes expressing NDI-related AQP2 proteins, these oocytes were analyzed in detail and were compared with wt AQP2-expressing oocytes. The stability of injected cRNA was equal for mutant

and wt AQP2 (Figure 3). In contrast, differences with wt AQP2 were observed on the protein level. Immunoblot analysis revealed that wt AQP2 was only expressed as a 29-kd protein, whereas the three mutants showed an additional 32-kd form (Figure 4). In a previous study on mutant AQP2 proteins similar 32-kd bands were detected, and they were shown to be endoglycosidase H-sensitive (17). Because endoglycosidase H hydrolyses endoplasmic reticulum-specific high-mannose glycosylation groups, the 32-kd bands presumably represent ER-retarded forms of mutant AQP2 proteins. The mutant AQP2 proteins are apparently retained in the endoplasmic reticulum and are thus impaired in their routing to the plasma membrane. The indication that the A147T-, T126M-, and N68S-substituted AQP2 proteins were impaired in their transport was further substantiated by the absence of these proteins in an immunoblotted oocyte fraction enriched for plasma membranes, whereas the wt AQP2 protein was clearly present (Figure 5). In addition, immunocytochemistry showed a clear AQP2 labeling in the plasma membrane of oocytes expressing wt AQP2, whereas the mutant AQP2 proteins were abundantly expressed in the cytoplasm, but were hardly detectable in the plasma membrane, which confirms the impaired transport of the mutant AQP2 proteins (Figure 6). In the ER, newly synthesized proteins undergo various post-translational modifications, including folding, oligomerization, and glycosylation (29,30). Proteins that are not properly processed do not pass the "quality control" of the ER and are usually retained. The processing of the new protein depends in part on the structural motifs displayed during folding and assembly, and by the molecular interactions with chaperones and folding factors. The quality control of the ER recognizes certain conformational features of the misfolded protein, such as hydrophobic peptide elements exposed on the surface of the molecule, and, in most cases, misprocessed proteins are subsequently degraded (29–31). In *Xenopus* oocytes, the stability of the T126M and N68S mutants was comparable with that of wt AQP2, but the A147T mutant was considerably less stable, a phenomenon previously shown for the S216P mutant also (17). Because the A147T and S216P mutations are both located in a transmembrane domain, misfolding may cause the exposure of hydrophobic regions on the surface of the molecule, which could make these mutants more accessible to ER-resident proteases. The other mutations (G64R, N68S, T126M, and R187C) are located in the more hydrophilic extramembranous loops, which may explain their stability in oocytes.

In summary, all six NDI-related missense AQP2 proteins (G64R, N68S, T126M, A147T, R187C, and S216P) are impaired in their transport to the plasma membrane when expressed in *Xenopus* oocytes (17; this study). Despite the impairment in routing, the A147T and T126M mutants significantly increased the Pf of oocytes. In view of the fact that the A147T mutant is very unstable in oocytes, the mutants that are stable in oocytes (G64R, N68S, and R187C) should also confer water permeability to oocytes, if they were functional water channels. Therefore, it is likely that the G64R, N68S and R187C AQP2 mutants are nonfunctional.

All of our data regarding AQP2 are in line with the hourglass model, which is a structural-functional model proposed for

AQP1. In this model, loops B and E are essential for the formation of the pore through which water transport takes place (32). The hourglass model is based on site-directed mutagenesis studies in which mutations in the B and E loops of AQP1, containing the conserved NPA boxes, resulted in loss of water permeability. Mutations in the A, C, and D loops and the N- and C-terminal regions, however, affected the water transporting properties of AQP1 to a lesser degree (33). All AQP2 proteins in NDI with mutations in the B loop (G64R, N68S) or E loop (R187C) are nonfunctional, whereas AQP2 proteins with mutations in the C loop (T126M) or near the D loop (A147T) are functional. Recently, Bai *et al.* (34) proposed that in AQP2 loops C and D are closely located to the aqueous pathway, instead of loops B and E. This is not in line with our data from NDI-related mutant AQP2 proteins. Bai *et al.* (34) reported that mutations near the NPA boxes in loops B and E did not alter water channel function, which contrasts sharply with our data.

In conclusion, two mutant AQP2 proteins, encoded by AQP2 genes of patients suffering from autosomal recessive NDI, appeared to be functional water channels. Therefore, the major cause underlying this disease is the misrouting of the mutant AQP2 proteins, and not the dysfunction of the water channels. As shown for the most common mutant form of the cystic fibrosis transmembrane conductance regulator (CFTR), which has a deletion of the phenylalanine at position 508, the primary effect is not a functional impairment, but rather an impairment in the routing of the mutant protein to the plasma membrane. In CFTR $\Delta$ F508-expressing cells it has been shown that culturing cells at lower temperatures relieved the impairment in routing of the  $\Delta$ F508 mutant, which resulted in the appearance of functional Cl<sup>-</sup> channels in the plasma membrane (35). Furthermore, elevated levels of molecular chaperones appeared to increase proper folding of the K304E mutant of the medium chain acyl-CoA dehydrogenase (MCAD) (36) and the Y393N mutation of the E1 $\alpha$  subunit of the mitochondrial branched chain  $\alpha$ -ketoacid dehydrogenase complex (37). In future studies, attempts should be undertaken to overcome the biosynthetic arrest and to promote trafficking of the T126M and A147T AQP2 mutants to subapical vesicles or the plasma membrane. This will require knowledge of the mechanism that causes retention. The opportunity to manipulate the cellular machinery associated with protein folding and trafficking may provide the tools for novel pharmacotherapeutic strategies that may be used in the treatment of this form of nephrogenic diabetes insipidus.

## Acknowledgments

We thank A. Hartog for performing immunocytochemistry on oocytes and Dr. R.J.M. Bindels for valuable suggestions. This study was supported by the Dutch Science Foundation (NWO-SLW-810-405-16.2) and the Dutch Kidney Foundation (C92.1262 and C93.1299)

## References

1. Preston GM, Carroll TP, Guggino WB, Agre P: Appearance of water channels in *Xenopus* oocytes expressing red cell CHIP28 protein. *Science* 256: 385–387, 1992

2. Fushimi K, Uchida S, Hara Y, Hirata Y, Marumo F, Sasaki S: Cloning and expression of apical membrane water channel of rat kidney collecting tubule. *Nature (Lond)* 361: 549–552, 1993
3. Echevarria M, Windhager EE, Tate SS, Frindt G: Cloning and expression of AQP3, a water channel from the medullary collecting duct of rat kidney. *Proc Natl Acad Sci USA* 91: 10997–11001, 1994
4. Ishibashi K, Sasaki S, Fushimi K, Uchida S, Kuwahara M, Saito H, Furukawa T, Nakajima K, Yamaguchi Y, Gojobori T, Marumo F: Molecular cloning and expression of a member of the aquaporin family with permeability to glycerol and urea in addition to water expressed at the basolateral membrane of kidney collecting duct cells. *Proc Natl Acad Sci USA* 91: 6269–6273, 1994
5. Ma T, Frigeri A, Hasegawa H, Verkman AS: Cloning of a water channel homolog expressed in brain meningeal cells and kidney collecting duct that functions as a stilbene-sensitive glycerol transporter. *J Biol Chem* 269: 21845–21849, 1994
6. Jung JS, Bhat RV, Preston GM, Guggino WB, Baraban JM, Agre P: Molecular characterization of an aquaporin cDNA from brain: Candidate osmoreceptor and regulator of water balance. *Proc Natl Acad Sci USA* 91: 13052–13056, 1994
7. Nielsen S, Smith BL, Christensen EI, Knepper MA, Agre P: CHIP28 water channels are localized in constitutively water-permeable segments of the nephron. *J Cell Biol* 120: 371–383, 1993
8. Katsura T, Verbavatz JM, Farinas J, Ma TH, Ausiello DA, Verkman AS, Brown D: Constitutive and regulated membrane expression of aquaporin 1 and aquaporin 2 water channels in stably transfected LLC-PK1 epithelial cells. *Proc Natl Acad Sci USA* 92: 7212–7216, 1995
9. Marples D, Knepper MA, Christensen EI, Nielsen S: Redistribution of aquaporin-2 water channels induced by vasopressin in rat kidney inner medullary collecting duct. *Am J Physiol* 38: C655–C664, 1995
10. Nielsen S, Chou CL, Marples D, Christensen EI, Kishore BK, Knepper MA: Vasopressin increases water permeability of kidney collecting duct by inducing translocation of aquaporin-CD water channels to plasma membrane. *Proc Natl Acad Sci USA* 92: 1013–1017, 1995
11. Sabolic I, Katsura T, Verbavatz JM, Brown D: The AQP2 water channel: Effect of vasopressin treatment, microtubule disruption, and distribution in neonatal rats. *J Membr Biol* 143: 165–175, 1995
12. Yamamoto T, Sasaki S, Fushimi K, Ishibashi K, Yaoita E, Kawasaki K, Marumo F, Kihara I: Vasopressin increases AQP-CD water channel in apical membrane of collecting duct cells in Brattleboro rats. *Am J Physiol* 268: C1546–C1551, 1995
13. Frigeri A, Gropper MA, Turck CW, Verkman AS: Immunolocalization of the mercurial-insensitive water channel and glycerol intrinsic protein in epithelial cell plasma membranes. *Proc Natl Acad Sci USA* 92: 4328–4331, 1995
14. Preston GM, Smith BL, Zeidel ML, Moulds JJ, Agre P: Mutations in aquaporin-1 in phenotypically normal humans without functional CHIP water channels. *Science* 265: 1585–1587, 1994
15. Deen PMT, Verdijk MA, Knoers NVAM, Wieringa B, Monnens LAH, van Os CH, van Oost BA: Requirement of human renal water channel aquaporin-2 for vasopressin-dependent concentration of urine. *Science* 264: 92–95, 1994
16. van Lieburg AF, Verdijk MA, Knoers VVAM, van Essen AJ, Proesmans W, Mallmann R, Monnens LAH, van Oost BA, van Os CH, Deen PMT: Patients with autosomal nephrogenic diabetes insipidus homozygous for mutations in the aquaporin 2 water-channel gene. *Am J Hum Genet* 55: 648–652, 1994
17. Deen PM, Croes H, van Aubel RA, Ginsel LA, van Os CH: Water channels encoded by mutant aquaporin-2 genes in nephrogenic diabetes insipidus are impaired in their cellular routing. *J Clin Invest* 95: 2291–2296, 1995
18. Hattori M, Sakaki Y: Dideoxy sequencing method using denatured plasmid templates. *Anal Biochem* 152: 232–238, 1986
19. Chomczynski P, Sacchi N: Single-step method of RNA isolation by acid guanidinium thiocyanate-phenol-chloroform extraction. *Anal Biochem* 162: 156–159, 1987
20. Deen PM, Dempster JA, Wieringa B, van Os CH: Isolation of a cDNA for rat CHIP28 water channel: High mRNA expression in kidney cortex and inner medulla. *Biochem Biophys Res Commun* 188: 1267–1273, 1992
21. Feinberg AP, Vogelstein B: A technique for radiolabeling DNA restriction endonuclease fragments to high specific activity. *Anal Biochem* 132: 6–13, 1983
22. Destree OH, Bendig MM, De Laaf RT, Koster JG: Organization of *Xenopus* histone gene variants within clusters and their transcriptional expression. *Biochim Biophys Acta* 782: 132–141, 1984
23. Wall DA, Patel S: Isolation of plasma membrane complexes from *Xenopus* oocytes. *J Membr Biol* 107: 189–201, 1989
24. Laemmli UK: Cleavage of structural proteins during the assembly of the head of bacteriophage T4. *Nature (Lond)* 227: 680–685, 1970
25. McLean IW, Nakane PK: Periodate-lysine-paraformaldehyde fixative. A new fixation for immunoelectron microscopy. *J Histochem Cytochem* 22: 1077–1083, 1974
26. Reizer J, Reizer A, Saier MHJ: The MIP family of integral membrane channel proteins: sequence comparisons, evolutionary relationships, reconstructed pathway of evolution, and proposed functional differentiation of the two repeated halves of the proteins. *Crit Rev Biochem Mol Biol* 28: 235–257, 1993
27. Knoers NVAM, van Os CH: Molecular and cellular defects in nephrogenic diabetes insipidus. *Curr Opin Nephrol Hypertens* 1996, in press.
28. Deen PM, Weghuis DO, Sinke RJ, Geurts van Kessel A, Wieringa B, van Os CH: Assignment of the human gene for the water channel of renal collecting duct Aquaporin 2 (AQP2) to chromosome 12 region q12→q13. *Cytogenet Cell Genet* 66: 260–262, 1994
29. Bonifacino JS, Lippincott Schwartz J: Degradation of proteins within the endoplasmic reticulum. *Curr Opin Cell Biol* 3: 592–600, 1991
30. Halban PA, Irminger JC: Sorting and processing of secretory proteins. *Biochem J* 299: 1–18, 1994
31. Hammond C, Helenius A: Quality control in the secretory pathway. *Curr Opin Cell Biol* 7: 523–529, 1995
32. Jung JS, Preston GM, Smith BL, Guggino WB, Agre P: Molecular structure of the water channel through aquaporin CHIP. The hourglass model. *J Biol Chem* 269: 14648–14654, 1994
33. Preston GM, Jung JS, Guggino WB, Agre P: Membrane topology of aquaporin CHIP. Analysis of functional epitope-scanning mutants by vectorial proteolysis. *J Biol Chem* 269: 1668–1673, 1994
34. Bai LQ, Fushimi K, Sasaki S, Marumo F: Structure of aquaporin-2 vasopressin water channel. *J Biol Chem* 271: 5171–5176, 1996
35. Denning GM, Anderson MP, Amara JF, Marshall J, Smith AE, Welsh MJ: Processing of mutant cystic fibrosis transmembrane conductance regulator is temperature-sensitive. *Nature (Lond)* 358: 761–764, 1992
36. Bross P, Andresen BS, Winter V, Kräutle F, Jensen TG, Nandy A, Kolvraa S, Ghisla S, Bolund I, Gregersen N: Co-overexpression of bacterial GroESL chaperonins partly overcomes non-productive folding and tetramer assembly of E. coli-expressed human medium-chain acyl-CoA dehydrogenase (MCAD) carrying the prevalent disease-causing K304E mutation. *Biochim Biophys Acta* 1182: 264–274, 1993
37. Thomas PJ, Qu BH, Pedersen PL: Defective protein folding as a basis of human disease. *Trends Biochem Sci* 20: 456–459, 1995